Dynamic Dipole and Quadrupole Phase Transitions in the Kinetic Metamagnetic Spin –3 / 2 Blume-Emery-Griffiths Model

Muharrem Kırak[a], Osman Canko[b], and Mustafa Keskin[b]

[a] Institute of Science, Erciyes University, 38039 Kayseri, Turkey
[b] Department of Physics, Erciyes University, 38039 Kayseri, Turkey

Reprint requests to M. K.; E-mail: keskin@erciyes.edu.tr

Z. Naturforsch. **64a,** 185 – 199 (2009); received August 28, 2008

We study, within a mean-field approach, the stationary states of the kinetic metamagnetic spin $-3/2$ Blume-Emery-Griffiths model under the presence of a time-varying (sinusoidal) magnetic field. We use the Glauber-type stochastic dynamics to describe the time evolution of the system. The behaviour of the time dependence of the average order parameters in a period, which are also called the dynamic order parameters, as functions of the reduced temperature are investigated. The natures (continuous or discontinuous) of the transitions are characterized by investigating the behaviours of the thermal variations of the dynamic order parameters. The dynamic phase transition points are obtained and the phase diagrams are constructed in the plane of the reduced temperature (T) and the amplitude of the magnetic field (h), and sixteen fundamental types of phase diagrams are found. The phase diagrams exhibit one, two, three or four dynamic tricritical points and a dynamic double-critical end point, and, besides a disordered and three ordered phases, seven coexistence regions or mixed phases depending on the interaction parameters. We also investigate the influence of the reduced biquadratic exchange parameter (k) and obtain nine different phase diagram topologies in the (k,T) plane.

Key words: Dynamic Phase Transition; Glauber-Type Stochastic Dynamics; Spin $-3/2$ Metamagnetic BEG Model; Dynamic Phase Diagrams.
PACS numbers: 05.50.+q; 05.70.Fh; 64.60.Ht; 75.10.Hk; 75.30.Kz; 75.50.Ee

1. Introduction

In our preceding paper [1], referred to as paper I in the following, we presented a study, within a mean-field approach, of the stationary states of the kinetic metamagnetic spin $-3/2$ Blume-Capel (BC) model in the presence of a time-dependent oscillating external magnetic field. We used the Glauber-type stochastic dynamics to describe the time evolution of the system. We have studied the time-dependent behaviour of the average submagnetizations in a period, which are also called the dynamic submagnetizations, as functions of the reduced temperature. The dynamic phase transition (DPT) points have been calculated by investigating the behaviour of the average submagnetizations in a period as functions of the reduced temperature. We presented the phase diagrams in the plane of the reduced temperature (T) and the amplitude of the magnetic field (h). We found six different phase diagram topologies. The system also exhibited one, two or three tricritical points depending upon the interaction parameters. We have investigated the influence of the reduced crystal-field interaction (d) and we obtain five different phase diagram topologies in the (d,T) plane. We have also studied the influence of the frequency on the phase boundaries as well as the dynamic tricritical point. We found that the topologies of the phase diagrams slightly change. In paper I, we did not study the influence of the biquadratic exchange interaction (K) due to the reason that the spin $-3/2$ BC model only contains a single-ion potential or crystal-field interaction in addition to the bilinear exchange interaction (J). The biquadratic exchange interaction is very important because it produces the ferroquadrupolar or simply the quadrupolar phase; hence, one has to consider the quadrupolar order parameters besides the magnetization. The purpose of the present paper is, therefore, to study within the mean-field approach the stationary states of the kinetic metamagnetic spin $-3/2$ Blume-Emery-Griffiths (BEG) model Hamiltonian with bilinear (J) and biquadratic (K) nearest-neighbour pair interactions and a single-ion potential or crystal-field interaction (D) in the presence of a time-dependent oscillating external magnetic field. We use the Glauber-type stochastic dy-

0932–0784 / 09 / 0300–0185 $ 06.00

namics to describe the time evolution of the system [2]. Especially, we investigate the time dependence of average submagnetizations and sublattice quadrupole moments, as well as the behaviour of the dynamic order parameters as functions of the reduced temperature. In these studies, we obtain the DPT points and construct the phase diagrams in the (T,h) plane. We also investigate the influence of the reduced biquadratic exchange interaction (k) and present the phase diagrams in the (k,T) plane.

It is worthwhile to mention that the existence of quadrupolar interactions has been established in several cubic rare-earth intermetallic compounds [3]. The most obvious proof is possibility of a quadrupolar phase transition, as observed for example in TmCd [4] and TmZn [5]. Moreover, the quadrupolar interactions may act on the nature of the magnetic phase transition in which they may change a second-order phase transition into a first-order one, as observed, e. g., in DySb [6], TbP [7] or TmCu [8], or vice versa as in $PrMg_2$ [9]. On the other hand, numerous theoretical works have been worked out concerning the existence of dipolar and quadrupolar phase transitions, especially in the Ising systems, such as spin -1 [10 – 12], spin $-3/2$ [13, 14] and spin -2 [15]. Magnetic dipolar and quadrupolar phase transitions in cubic rare-earth intermetallic compounds have been studied in terms of single-ion susceptibilities and within the Landau theory [16]. Recently, the quadrupolar order in the $S=1$ isotropic Heisenberg model with the biquadratic interaction has been studied by the quantum Monte Carlo simulation [17].

On the other hand, metamagnetic systems are systems with both ferromagnetic and antiferromagnetic couplings; they are of great interest because it is possible to induce novel kinds of critical behaviour by forcing competition between these couplings, especially by applying a magnetic field. $FeCl_2$, $FeBr_2$, La_2CuO_4, $Ni(NO_3)_2{\cdot}2H_2O$, dysprosium aluminum garnet (DAG) etc. are well known metamagnets. The equilibrium behaviours of these metamagnets have been studied in detail [18]. While equilibrium properties of Ising metamagnets have been investigated extensively, the dynamical aspects of the metamagnets have not been thoroughly explored [1]. Hence, it would also be of interest to learn some ething about the dynamical properties of the metamagnets.

Finally, we should also mention that the DPT presents new challenges and there is a strong motivation for analyzing it; hence, the DPT has attracted much attention in recent years, theoretically [19]. Experimental evidence for the DPT has been found in magnetic systems [20] and amorphous YBaCuO films [21]. Besides the scientific interests, the study of the DPT can inspire new methods in materials manufacturing and processing, and interesting methods in nanotechnology, such as pattern formation [22], monomolecular organic films [23], beam-induced transformation and many others [23]. Moreover, the DPT may have played a role in the evolution of the early universe [24].

The outline of the remaining part of this paper is organized as follows. In Section 2, the metamagnetic spin $-3/2$ BEG model is presented briefly. In Section 3, the derivation of the mean-field dynamic equations of motion by using the Glauber-type stochastic dynamics in the presence of a time-dependent oscillating external magnetic field is given. In Section 4, the stationary solutions of the coupled dynamic equations are solved and the thermal behaviours of the dynamic submagnetizations and dynamic sublattice quadrupole moments are studied, and, as a result, the DPT points are calculated. Section 5 contains the presentation and discussion of the phase diagrams. Finally, the paper ends with a summary and conclusions of this work in Section 6.

2. The Metamagnetic Spin –3/2 BEG Model

The magnetic moments or spins are arranged on a regular lattice of N sites that consist of two equivalent interpenetrating sublattices, denoted by A and B, each having a total of $N/2$ sites. The z nearest neighbours (nn) of every spin on a particular sublattice are all on the other sublattice, precisely, each A-site is surrounded by z equilavent neighbouring B-sites and each B-site by z A-sites. On the other hand, the z' next-nearest neighbours (nnn) of every spin are all on the same lattice, namely, the number of any A-sites closest to any given A-site or the number of any B-sites closest to any given B-site is z'. Hence, for example $z=4$ and $z'=4$ for the plane square lattice and $z=6$ and $z'=12$ for the simple cubic lattice. Nevertheless, in the mean-field approach the only relevant properties of the lattice structure that enter are z and z' in Section 3.

The metamagnetic spin $-3/2$ BEG model in the presence of a time-dependent oscillating external magnetic field is defined by the Hamiltonian

$$\mathcal{H} = -J\sum_{\mathrm{nn}} S_i S_j - J'\sum_{\mathrm{nnn}} S_i S_k$$

$$
\begin{aligned}
&- D\left(\sum_{i=1}^{N} S_i^2 + \sum_{j=1}^{N} S_j^2\right) \\
&- K\sum_{\mathrm{nn}} (S_i^2 - 5/4)(S_j^2 - 5/4) \\
&- K'\sum_{\mathrm{nnn}} (S_i^2 - 5/4)(S_k^2 - 5/4) \\
&- H\left(\sum_{i=1}^{N} S_i + \sum_{j=1}^{N} S_j\right), \qquad (1)
\end{aligned}
$$

where the spin S_i takes the values $\pm 3/2$ or $\pm 1/2$ at each i site of lattice, $\sum_{\mathrm{nn}}$ and $\sum_{\mathrm{nnn}}$ are sums over all pairs of nn and nnn spins, respectively, J and J' are bilinear exchange constants for the nn and nnn, and K and K' are biquadratic exchange constants for the nn and nnn, respectively. D is the crystal-field interaction or single-ion anisotropy constant and H is a time-dependent external oscillating magnetic field: $H(t) = \cos(wt)$, where H_0 and $w = 2\pi\nu$ are the amplitude and the angular frequency of the oscillating field, respectively. The system is in contact with an isothermal heat bath at absolute temperature T.

The order parameters of the system are introduced as follows: (1) The average submagnetizations $m_{\mathrm{A}} \equiv \langle S\rangle_{\mathrm{A}}$ and $m_{\mathrm{B}} \equiv \langle S\rangle_{\mathrm{B}}$, which are the excess of one orientation over the other orientations, also called dipole moments. (2) The sublattice quadrupole moments (q_{A} and q_{B}), which are linear functions of the average squared submagnetizations, i. e., $q_{\mathrm{A}} \equiv \langle S^2 - 5/4\rangle_{\mathrm{A}}$ and $q_{\mathrm{B}} \equiv \langle S^2 - 5/4\rangle_{\mathrm{B}}$, which are different from the definition $q \equiv \langle S^2\rangle$ used by some researchers [18]. The first definition ensures $q = 0$ at infinite temperature.

3. Derivation of the Mean-Field Dynamic Equations

Since derivation of the mean-field dynamic equations is discussed in paper I extensively, we will only give a brief summary here. The system evolves according to the Glauber-type stochastic process at a rate of $1/\tau$ transitions per unit time. We define $p(S_1, S_2, \ldots, S_N; t)$ as the probability that the system has the S spin configuration, $S_1, S_2, \ldots, S_N$, at time t. The time dependence of this probability function is assumed to be governed by the master equation which describes the interaction between the spins and the heat bath. In the Glauber dynamics, the transition probabilities of the individual spins are assumed to depend on the momentary values of the neighbouring spins as well as on the influence of the heat bath and $W_i(S_i \to S_i')$ is the probability per unit time that the i-th spin changes from S_i to S_i' while the other values remain momentarily fixed. Therefore, if the spins on sublattice B remain momentarily fixed, the master equation for sublattice A can be written as

$$
\begin{aligned}
&\frac{\mathrm{d}}{\mathrm{d}t} P_{\mathrm{A}}(S_1, S_2, \ldots, S_N; t) = \\
&-\sum_i \left(\sum_{S_i^1 S_i'} W_{i_{\mathrm{A}}}(S_i \to S_i')\right) P_{\mathrm{A}}(S_1, S_2, \ldots, S_i, \ldots, S_N; t) \\
&+\sum_i \left(\sum_{S_i^1 S_i'} W_{i_{\mathrm{A}}}(S_i' \to S_i) P_{\mathrm{A}}(S_1, S_2, ..., S_i', ..., S_N; t)\right), \qquad (2)
\end{aligned}
$$

where $W_{i_{\mathrm{A}}}(S_i \to S_i')$ and $W_{i_{\mathrm{A}}}(S_i' \to S_i)$ are the probabilities per unit time that the i-th spin changes from S_i to S_i' and S_i' to S_i, respectively. Since the system is in contact with a heat bath at absolute temperature T, each spin can change from S_i to S_i' with the probability per unit time

$$
W_{i_{\mathrm{A}}}(S_i \to S_i') = \frac{1}{\tau} \frac{\exp(-\beta \Delta E_{\mathrm{A}}(S_i \to S_i'))}{\sum_{S_i'} \exp(-\beta \Delta E_{\mathrm{A}}(S_i \to S_i'))}, \qquad (3)
$$

where $\beta = 1/k_{\mathrm{B}}T$, k_{B} is the Boltzmann factor, $\sum_{S_i'}$ is the sum over the four possible values of S_i', $\pm 3/2$, $\pm 1/2$, and

$$
\begin{aligned}
\Delta E_{\mathrm{A}}(S_i \to S_i') &= -(S_i' - S_i)\left(H + J\sum_{\mathrm{nn}} S_j + J'\sum_{\mathrm{nnn}} S_k\right) \\
&-(S_i'^2 - S_i^2)\left(D + K\sum_{\mathrm{nn}} \left(S_j^2 - \frac{5}{4}\right) + K'\sum_{\mathrm{nnn}} \left(S_k^2 - \frac{5}{4}\right)\right) \qquad (4)
\end{aligned}
$$

gives the change in the energy of the system when the S_i spin changes. The probabilities satisfy the detailed balance condition. Since $W_{i_{\mathrm{A}}}(S_i \to S_i')$ does not depend on S_i, we can write $W_{i_{\mathrm{A}}}(S_i \to S_i') = W_{i_{\mathrm{A}}}(S_i')$. Hence the master equation becomes

$$
\begin{aligned}
&\frac{\mathrm{d}}{\mathrm{d}t} P_{\mathrm{A}}(S_1, S_2, \ldots, S_N; t) = \\
&-\sum_i \left(\sum_{S_i'^1 S_i} W_{i_{\mathrm{A}}}(S_i')\right) P_{\mathrm{A}}(S_1, S_2, \ldots, S_i, \ldots, S_N; t) \\
&+\sum_i W_{i_{\mathrm{A}}}(S_i) \left(\sum_{S_i'^1 S_i} P_{\mathrm{A}}(S_1, S_2, \ldots, S_i', \ldots, S_N; t)\right). \qquad (5)
\end{aligned}
$$

Since the sum of the probabilities is normalized to one, by multiplying both sides of (5) with S_k for m_{A} and $(S_k^2 - 5/4)$ for q_{A}, and taking the average, we obtain

$$\tau\frac{\mathrm{d}}{\mathrm{d}t}\langle S_i\rangle_{\mathrm{A}} = -\langle S_i\rangle_{\mathrm{A}} + \left\langle \frac{3\exp(\beta y)\sinh(3\beta x/2)+\exp(-\beta y)\sinh(\beta x/2)}{2\exp(\beta y)\cosh(3\beta x/2)+2\exp(-\beta y)\cosh(\beta x/2)} \right\rangle, \tag{6}$$

$$\tau\frac{\mathrm{d}}{\mathrm{d}t}\langle S_i^2-5/4\rangle_{\mathrm{A}} = -\langle S_i^2-5/4\rangle_{\mathrm{A}} + \left\langle \frac{\exp(\beta y)\cosh(3\beta x/2)-\exp(-\beta y)\cosh(\beta x/2)}{\exp(\beta y)\cosh(3\beta x/2)+\exp(-\beta y)\cosh(\beta x/2)} \right\rangle, \tag{7}$$

where $x = J\sum_{\mathrm{nn}} S_j + J'\sum_{\mathrm{nnn}} S_k + H$ and $y = D + K\sum_{\mathrm{nn}}(S_j^2-5/4) + K'\sum_{\mathrm{nnn}}(S_k^2-5/4)$.

Using the mean-field approach, we obtain the following set of mean-field dynamical equations of motion for the order parameters in the presence of a time-varying field:

$$\Omega\frac{\mathrm{d}}{\mathrm{d}\xi}m_{\mathrm{A}} = -m_{\mathrm{A}} + \frac{3\exp(a_2/T)\sinh[3a_1/2\alpha T]+\exp(-a_2/T)\sinh[a_1/2\alpha T]}{2\exp(a_2/T)\cosh[3a_1/2\alpha T]+2\exp(-a_2/T)\cosh[a_1/2\alpha T]}, \tag{8}$$

$$\Omega\frac{\mathrm{d}}{\mathrm{d}\xi}q_{\mathrm{A}} = -q_{\mathrm{A}} + \frac{\exp(a_2/T)\cosh[3a_1/2\alpha T]-\exp(-a_2/T)\cosh[a_1/2\alpha T]}{\exp(a_2/T)\cosh[3a_1/2\alpha T]+\exp(-a_2/T)\cosh[a_1/2\alpha T]}, \tag{9}$$

where $\alpha = \mathcal{J}'/\mathcal{J}$ $(\mathcal{J} = Jz, \mathcal{J}' = J'z')$, $k = \mathcal{K}/\mathcal{J}'$, $k' = \mathcal{K}'/\mathcal{J}'$ $(\mathcal{K} = Kz, \mathcal{K}' = K'z')$, $d = D/\mathcal{J}'$, $a_1 = m_{\mathrm{B}} + \alpha m_{\mathrm{A}} + \alpha h\cos(\xi)$, $\xi = wt$, $a_2 = \alpha d + q_{\mathrm{B}}k + q_{\mathrm{A}}k'$, $m_{\mathrm{A}} \equiv \langle S\rangle_{\mathrm{A}}$, $m_{\mathrm{B}} \equiv \langle S\rangle_{\mathrm{B}}$, $q_{\mathrm{A}} \equiv \langle S^2-5/4\rangle_{\mathrm{A}}$, $q_{\mathrm{B}} \equiv \langle S^2-5/4\rangle_{\mathrm{B}}$, $T = (\beta\mathcal{J}')^{-1}$, $h = H_0/\mathcal{J}'$ and $\Omega = \tau w$.

Now, assuming that the spins on sublattice A remain momentarily fixed and the spins on the sublattice B change, we obtain the mean-field dynamical equation for the submagnetization m_{B} with the similar calculation as

$$\Omega\frac{\mathrm{d}}{\mathrm{d}\xi}m_{\mathrm{B}} = -m_{\mathrm{B}} + \frac{3\exp(b_2/T)\sinh[3b_1/2\alpha T]+\exp(-b_2/T)\sinh[b_1/2\alpha T]}{2\exp(b_2/T)\cosh[3b_1/2\alpha T]+2\exp(-b_2/T)\cosh[b_1/2\alpha T]}, \tag{10}$$

$$\Omega\frac{\mathrm{d}}{\mathrm{d}\xi}q_{\mathrm{B}} = -q_{\mathrm{B}} + \frac{\exp(b_2/T)\cosh[3b_1/2\alpha T]-\exp(-b_2/T)\cosh[b_1/2\alpha T]}{\exp(b_2/T)\cosh[3b_1/2\alpha T]+\exp(-b_2/T)\cosh[b_1/2\alpha T]}, \tag{11}$$

where $b_1 = m_{\mathrm{A}} + \alpha m_{\mathrm{B}} + \alpha h\cos\xi$ and $b_2 = \alpha d + q_{\mathrm{A}}k + q_{\mathrm{B}}k'$. Hence, the set of mean-field dynamical equations for the order parameters is obtained. We fixed $J = -1.00$ and $\Omega = 2\pi$. The solutions and discussion of these equations are given in the next section.

4. Thermal Behaviours of Dynamic Order Parameters and Dynamic Phase Transition Points

In this section, we will first solve the set of dynamic equations and present the time variation of the average order parameters. Then we will obtain the average order parameters in a period, which are also called the dynamic order parameters, and investigate and present the thermal behaviour of the dynamic order parameters as functions of the reduced temperature, and as a result, the DPT points will be calculated. For these purposes, first we have to study the stationary solutions of the set of dynamic equations, given in (8)–(11), if the parameters T, k, k', d, α, α and h are varied. The stationary solutions of (8)–(11) will be periodic functions of ξ with period 2π; that is, $m_{\mathrm{A}}(\xi+2\pi) = m_{\mathrm{A}}(\xi)$, $m_{\mathrm{B}}(\xi+2\pi) = m_{\mathrm{B}}(\xi)$, $q_{\mathrm{A}}(\xi+2\pi) = q_{\mathrm{A}}(\xi)$ and $q_{\mathrm{B}}(\xi+2\pi) = q_{\mathrm{B}}(\xi)$. Moreover, they can be one of three types according to whether they have or do not have the properties

$$m_{\mathrm{A}}(\xi+\pi) = -m_{\mathrm{A}}(\xi), \quad m_{\mathrm{B}}(\xi+\pi) = -m_{\mathrm{B}}(\xi) \tag{12a}$$

and

$$q_{\mathrm{A}}(\xi+\pi) = -q_{\mathrm{A}}(\xi), \quad q_{\mathrm{B}}(\xi+\pi) = -q_{\mathrm{B}}(\xi). \tag{12b}$$

The first type of solution, satisfying both (12a) and (12b), is called a symmetric solution. It corresponds to a disordered (d) solution. In this solution, the average submagnetizations, namely m_{A} and m_{B}, always oscillate around zero value and are delayed with respect to the external magnetic field. On the other hand, the sublattice quadrupolar moments, namely q_{A} and q_{B}, are equal to each other ($q_{\mathrm{A}} = q_{\mathrm{B}}$) but oscillate around a nonzero value for finite temperature.

The second type of solution, which does not satisfy both (12a) and (12b), is called a nonsymmetric

solution. m_A and m_B do not follow the external magnetic field any more, but instead of oscillating around zero value, they oscillate around a nonzero value, namely $\pm 3/2$ or $\pm 1/2$.

The third type of solution, which satisfies (12a) but does not satisfy (12b), corresponds to a ferroquadrupolar or simply quadrupolar (fq) phase. m_A and m_B oscillate around zero and are delayed with respect to the external magnetic field; q_A and q_B do not follow the external magnetic field any more. A nonsymmetric solution leads to the following three different phases or solutions depending on the oscillating of the sublattice order parameters:

1. The antiferromagnetic $-3/2$ phase ($af_{3/2}$): $m_A = -m_B = \pm 3/2$ and $q_A = q_B \neq 0$.
2. The antiferromagnetic $-1/2$ phase ($af_{1/2}$): $m_A = -m_B = \pm 1/2$ and $q_A = q_B \neq 0$.
3. The ferroquadrupolar phase (fq): $m_A = m_B = 0$ and $q_A = q_B = -1$.

These above facts are seen explicitly by solving (8)–(11) numerically using the numerical method of the Adams-Moulton predictor corrector method for a given set of parameters and initial values; the solutions are presented in Figure 1. From Fig. 1, one can see five different solutions, namely the d, $af_{3/2}$, $af_{1/2}$ and fq phases or solutions and a coexistence solution, namely the $af_{3/2} + af_{1/2}$ in which $af_{3/2}$, $af_{1/2}$ solutions coexist. In Fig. 1a, only the symmetric solution is obtained; hence, we have a disordered (d) solution. In Figs. 1b, c and d only the nonsymmetric solutions are found; therefore, we have the $af_{3/2}$, $af_{1/2}$ and fq solutions, respectively. These solutions do not depend on the initial values. In Fig. 1e, we have also the nonsymmetric solution for $m_A(\xi)$, $m_B(\xi)$, $q_A(\xi)$ and $q_B(\xi)$, because $m_A(\xi)$ and $m_B(\xi)$ oscillate around either $+3/2$ or $+1/2$ and $-3/2$ or $-1/2$ at $T = 0$ and $q_A(\xi) = q_B(\xi)$ oscillate around $+1$ or -1 at $T = 0$, respectively. Hence, we have the solution coexistence ($af_{3/2} + af_{1/2}$). In this case, the solution depends on the initial values, as seen in Fig. 1e explicitly. Similarly, we have the $af_{1/2}$ + fq, $af_{3/2}$ + fq, $af_{3/2}$ + d, $af_{3/2} + af_{1/2}$ + fq, fq + d, and $af_{3/2}$ + fq + d coexistence solutions. We should also mention that these solutions depend on the initial values. Since these solutions or phases are similar to those in Fig. 1e, we do not present these phases. In order to see the dynamic phase boundaries among these phases, we have to calculate DPT points, and then we can present dynamic phase diagrams of the system. DPT points are obtained by investigating the behaviour of the dynamic order parameters as functions of the reduced temperature.

The dynamic order parameters, namely, the dynamic sublattice magnetizations (M_A and M_B) and the dynamic sublattice quadrupole moments (Q_A and Q_B), are defined as

$$M_A = \frac{1}{2\pi}\int_0^{2\pi} m_A(\xi)\mathrm{d}\xi, \quad M_B = \frac{1}{2\pi}\int_0^{2\pi} m_B(\xi)\mathrm{d}\xi \quad (13a)$$

and

$$Q_A = \frac{1}{2\pi}\int_0^{2\pi} q_A(\xi)\mathrm{d}\xi, \quad Q_B = \frac{1}{2\pi}\int_0^{2\pi} q_B(\xi)\mathrm{d}\xi. \quad (13b)$$

The behaviours of M_A, M_B and Q_A, Q_B as functions of the reduced temperature for several values of k, k', d, α and h are obtained by combining the numerical methods of Adams-Moulton predictor corrector with the Romberg integration. We give a few interesting examples to illustrate the calculation of the DPT points (seen in Fig. 2). In these figures, thick lines represent M_A and M_B, and thin lines represent Q_A and Q_B. TC (thick arrow) is the second-order phase transition temperature from the $af_{3/2}$ phase to the d phase, $T_{C'}$ (thin arrow) is from the $af_{1/2}$ phase to the fq phase. T_t represents the first-order phase transition temperature for M_A, M_B, Q_A and Q_B. In addition to this, T_{tQ} is the first-order phase transition temperatures for only Q_A and Q_B. Figure 2a shows the reduced temperature dependence of the dynamic order parameters for $k = k' = 0.10$, $d = -0.06$, $\alpha = -0.75$, and $h = 0.50$. In this figure, $M_A = 3/2$, $M_B = -3/2$ and $Q_A = Q_B = 1.0$ at zero temperature; M_A and $Q_A = Q_B$ decrease and M_B increases to zero continuously as the reduced temperature increases. Therefore, the second-order phase transition occurs ($T_C = 2.09$) and the phase transition is from the $af_{3/2}$ phase to the d phase (compare Fig. 2a with Fig. 3a for $h = 0.50$). Figure 2b shows the behaviours of M_A, M_B and Q_A, Q_B as functions of the reduced temperature for $k = k' = 0.05$, $d = -0.75$, $\alpha = -0.05$, and $h = 0.25$. $M_A = 1/2, M_B = -1/2$ and $Q_A = Q_B = -1.0$ at zero temperature and the system exhibits a second-order phase transition and the transition is from the $af_{1/2}$ phase to the fq phase ($T_{C'} = 0.23$) (compare Fig. 2b with Fig. 3g for $h = 0.25$). Figures 2c and d illustrate the thermal variations of dynamic order parameters for $k = k' = 1.00$, $d = 0.025$, $\alpha = -0.10$, and $h = 0.125$ for two different initial values; i. e.,

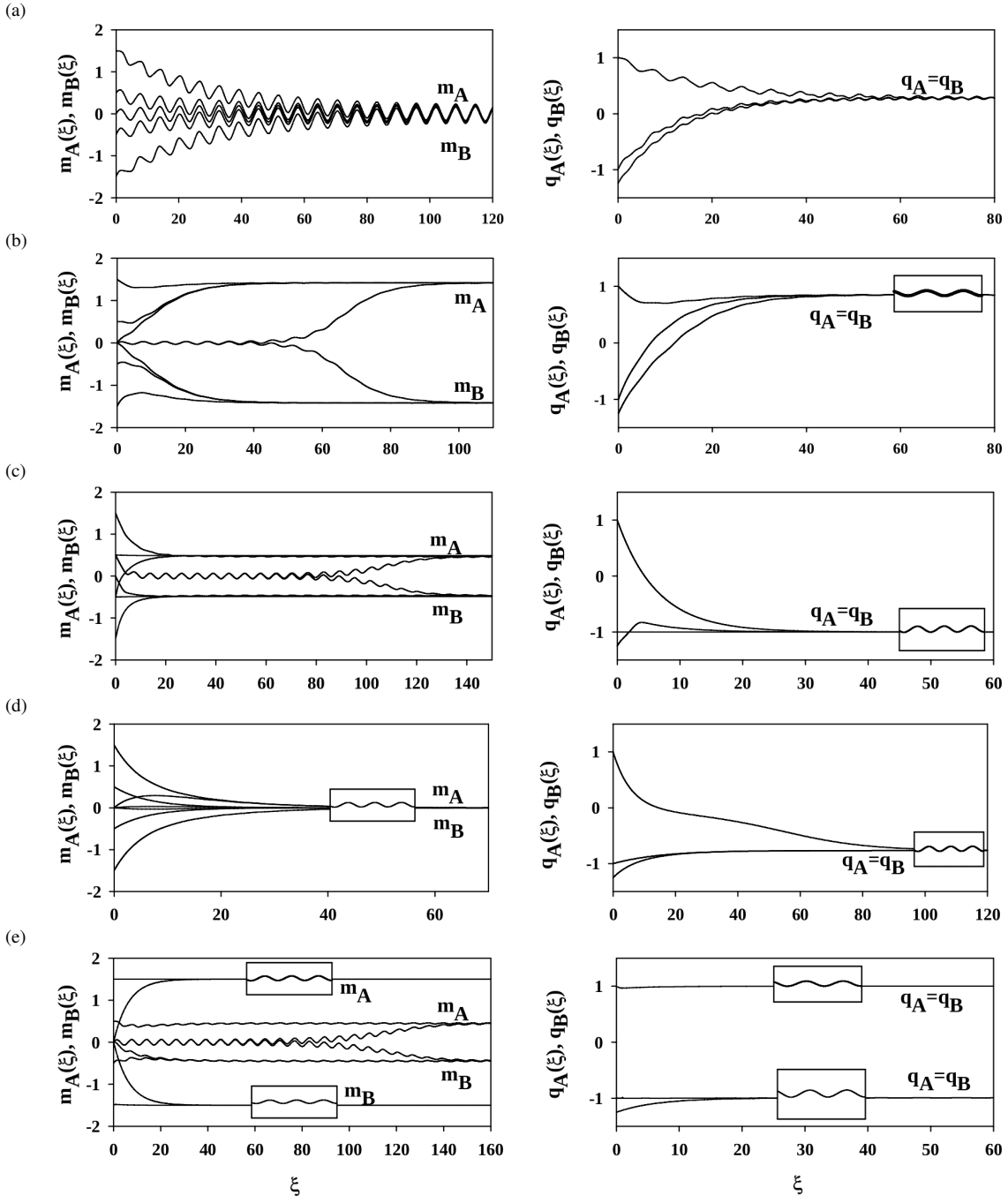

Fig. 1. Time variations of the sublattice magnetizations (m_A and m_B) and sublattice quadrupole moments (q_A and q_B): (a) a disordered (d) phase for $k = k' = 0.50$, $d = -0.25$, $\alpha = -1.00$, $h = 2.50$, and $T = 2.00$; (b) an antiferromagnetic $-3/2$ ($af_{3/2}$) phase for $k = k' = 0.10$, $d = -0.06$, $\alpha = -0.75$, $h = 0.18$, and $T = 1.03$; (c) an antiferromagnetic $-1/2$ ($af_{1/2}$) phase for $k = k' = 0.25$, $d = -0.56$, $\alpha = -0.10$, $h = 0.25$, and $T = 0.125$; (d) a ferroquadrupolar (fq) phase for $k = k' = 1.50$, $d = 0.025$, $\alpha = -0.10$, $h = 0.025$, and $T = 2.25$; (e) a coexistence region ($af_{3/2} + af_{1/2}$) for $k = k' = 0.50$, $d = -0.25$, $\alpha = -1.00$, $h = 0.50$, and $T = 0.25$.

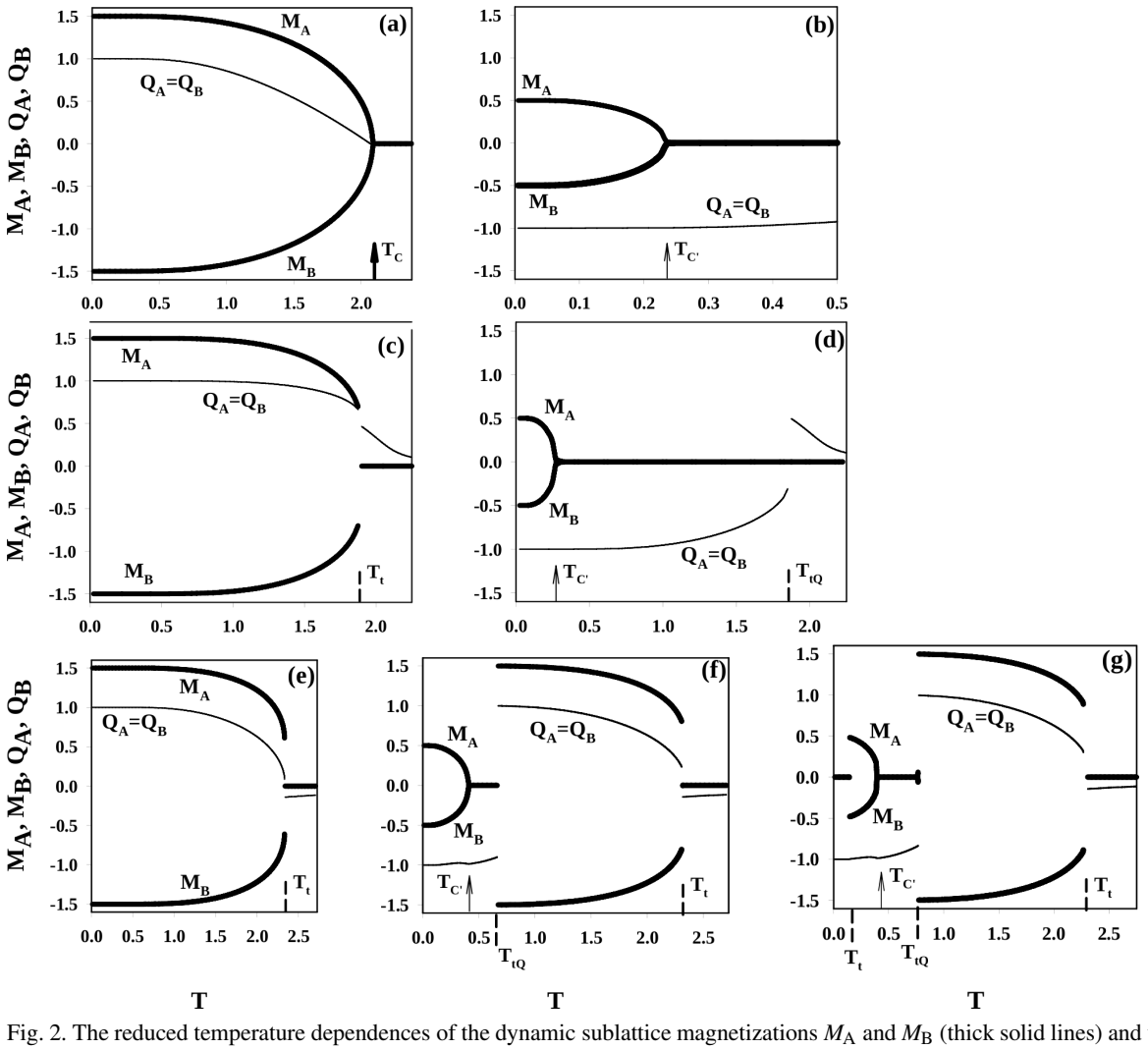

Fig. 2. The reduced temperature dependences of the dynamic sublattice magnetizations M_A and M_B (thick solid lines) and the dynamic sublattice quadrupole moments Q_A and Q_B (thin solid lines). T_C (thick arrow) is the second-order phase transition temperature from the af$_{3/2}$ phase to the d phase; $T_{C'}$ (thin arrow) is from the af$_{1/2}$ phase to the fq phase. T_t represents the first-order phase transition temperature for M_A, M_B, Q_A and Q_B. T_{tQ} is the first-order phase transition temperature for only Q_A and Q_B. (a) Second-order phase transition from the af$_{3/2}$ phase to the d phase for $k = k' = 0.10$, $d = -0.06$, $\alpha = -0.75$, and $h = 0.50$; 2.09 is found to be T_C. (b) Second-order phase transition from the af$_{1/2}$ phase to the fq phase for $k = k' = 0.05$, $d = -0.75$, $\alpha = -0.05$, and $h = 0.25$; 0.23 is found to be $T_{C'}$. (c) First-order phase transition from the af$_{3/2}$ phase to the d phase for $k = k' = 1.00$, $d = 0.025$, $\alpha = -0.10$, and $h = 0.125$; 1.89 is found to be T_t. (d) Two successive phase transitions: the first one is a second-order phase transition from the af$_{1/2}$ phase to the fq phase and the second one is a first-order phase transition from the fq phase to the d phase for $k = k' = 1.00$, $d = 0.025$, $\alpha = -0.10$, and $h = 0.125$; 0.27 and 1.85 are found to be $T_{C'}$ and T_{tQ}, respectively. (e) First-order phase transition from the af$_{3/2}$ phase to the fq phase for $k = k' = 0.50$, $d = -0.25$, $\alpha = -1.20$, and $h = 0.75$; 2.34 is found to be T_t; (f) Three successive phase transitions: the first one is a second-order phase transition from the af$_{1/2}$ phase to the fq phase, the second one is a first-order phase transition from the fq phase to the af$_{3/2}$ phase, and the third one is also a first-order phase transition from the af$_{3/2}$ phase to the fq phase for $k = k' = 0.50$, $d = -0.25$, $\alpha = -1.20$, and $h = 0.75$; 0.41, 0.67, and 2.31 are found to be $T_{C'}$, T_{tQ}, and T_t, respectively. (g) Four successive phase transitions: the first one is a first-order phase transition from the fq phase to the af$_{1/2}$ phase, the second one is a second-order phase transition from the af$_{1/2}$ phase to the fq phase, the third one is a first-order phase transition from the fq phase to the af$_{3/2}$ phase and the fourth one is also a first-order phase transition from the af$_{3/2}$ phase to the fq phase for $k = k' = 0.50$, $d = -0.25$, $\alpha = -1.20$, and $h = 0.75$; 0.14, 0.41, 0.67, and 2.31 are found T_t, $T_{C'}$, T_{tQ}, and T_t, respectively.

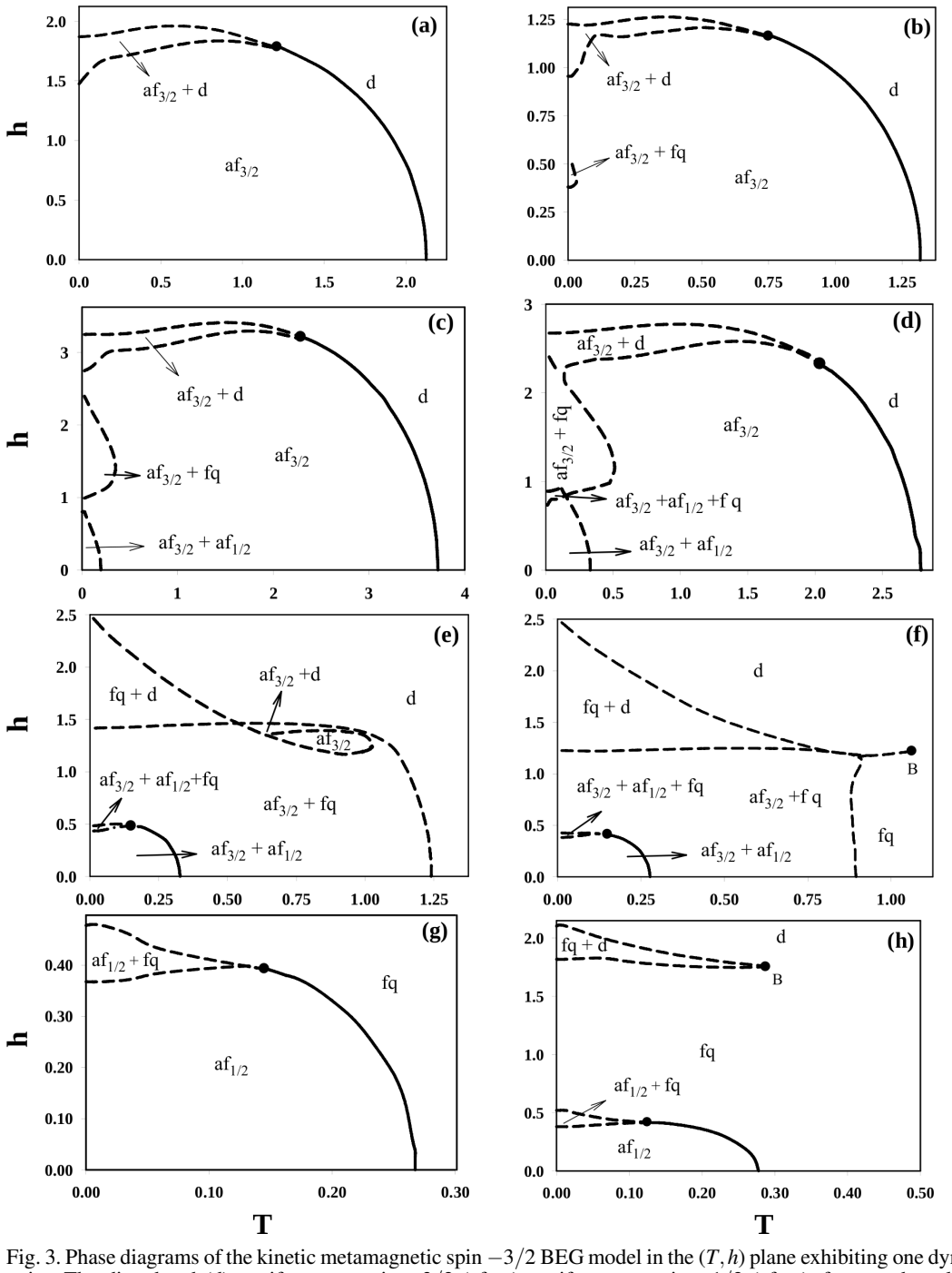

Fig. 3. Phase diagrams of the kinetic metamagnetic spin $-3/2$ BEG model in the (T,h) plane exhibiting one dynamic tricritical point. The disordered (d), antiferromagnetic $-3/2$ ($af_{3/2}$), antiferromagnetic $-1/2$ ($af_{1/2}$), ferroquadrupolar (fq), and six different regions of coexisting phases, namely, the $af_{3/2}+af_{1/2}$, $af_{3/2}+af_{1/2}+fq$, $af_{3/2}+fq$, $af_{3/2}+d$, $af_{1/2}+fq$ and $fq+d$ regions, are found. Dashed and solid lines represent the first- and second-order phase transitions, respectively, the dynamic tricritical point is indicated with filled circles, and B denotes the dynamic double-critical end point. (a) $k=k'=0.10$, $d=-0.06$, $\alpha=-0.75$; (b) $k=k'=0.10$, $d=-0.06$, $\alpha=-0.15$; (c) $k=k'=0.50$, $d=-0.25$, $\alpha=-2.20$; (d) $k=k'=0.50$, $d=-0.25$, $\alpha=-1.50$; (e) $k=k'=0.50$, $d=-0.25$, $\alpha=-0.30$; (f) $k=k'=0.50$, $d=-0.25$, $\alpha=-0.10$; (g) $k=k'=0.05$, $d=-0.75$, $\alpha=-0.05$; (h) $k=k'=0.25$, $d=-0.56$, $\alpha=-0.10$.

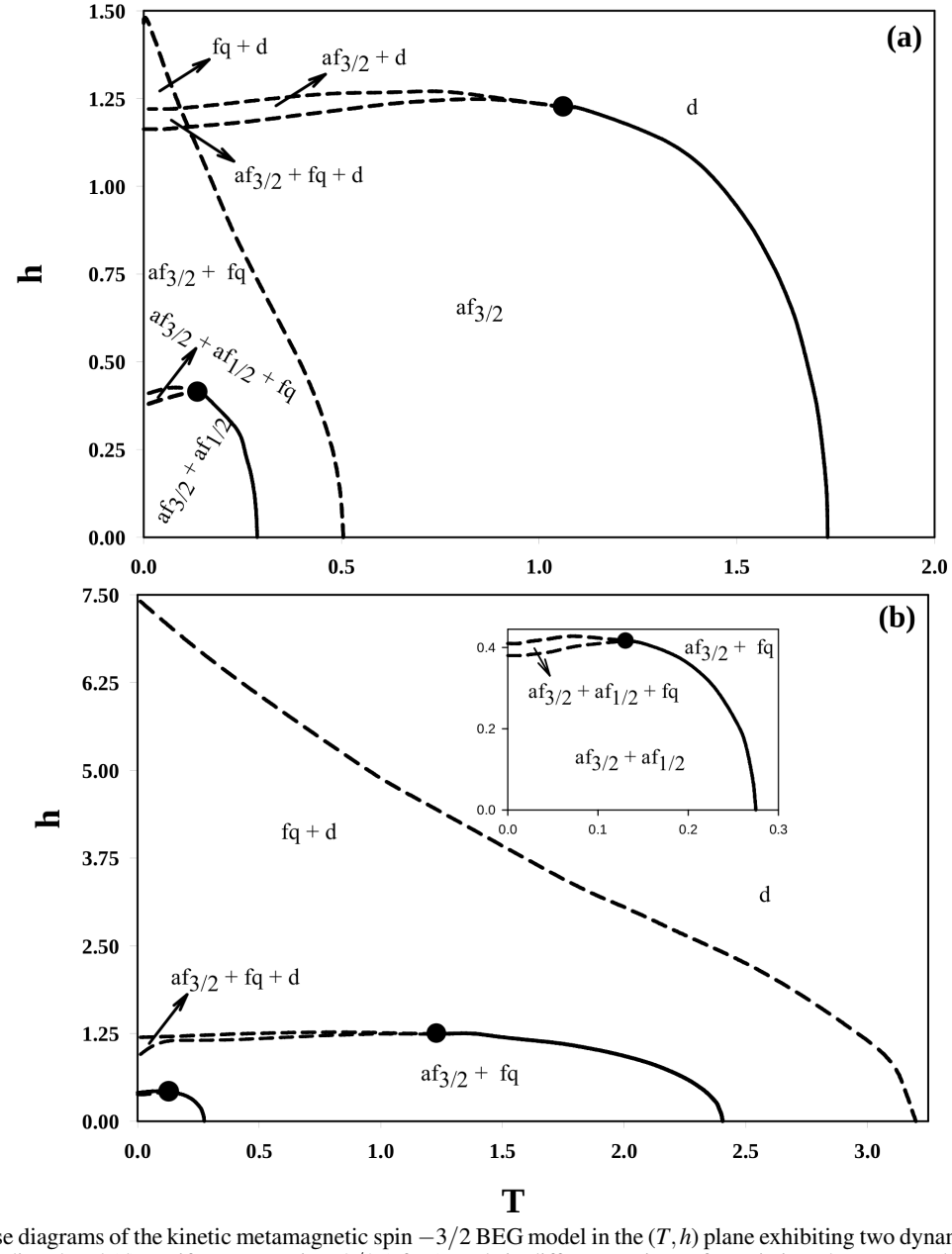

Fig. 4. Phase diagrams of the kinetic metamagnetic spin −3/2 BEG model in the (T, h) plane exhibiting two dynamic tricritical points. The disordered (d), antiferromagnetic −3/2 ($af_{3/2}$), and six different regions of coexisting phases, namely, the $af_{3/2} + af_{1/2}$, $af_{3/2} + af_{1/2} + fq$, $af_{3/2} + fq$, $af_{3/2} + d$, $af_{3/2} + fq + d$ and $fq + d$ regions, are found. Dashed and solid lines represent the first- and second-order phase transitions, respectively, the dynamic tricritical points are indicated with filled circles. (a) $k = k' = 0.50$, $d = 0.25$, $\alpha = -0.10$; (b) $k = k' = 2.00$, $d = 0.25$, $\alpha = -0.10$.

$M_A = 3/2$, $M_B = 0.0$, $Q_A = 1.0$, and $Q_B = -1.25$ for Fig. 2c and $M_A = 1/2$, $M_B = 0.0$, $Q_A = -1.0$, and $Q_B = -1.25$ for Figure 2d. Figure 2c shows that M_A, M_B and $Q_A = Q_B$ undergo a first-order phase transition, because M_A and $Q_A = Q_B$ decrease and M_B increases to zero discontinuously as the temperature increases. The system undergoes the first-order phase transition that is from the $af_{3/2}$ phase to the d phase

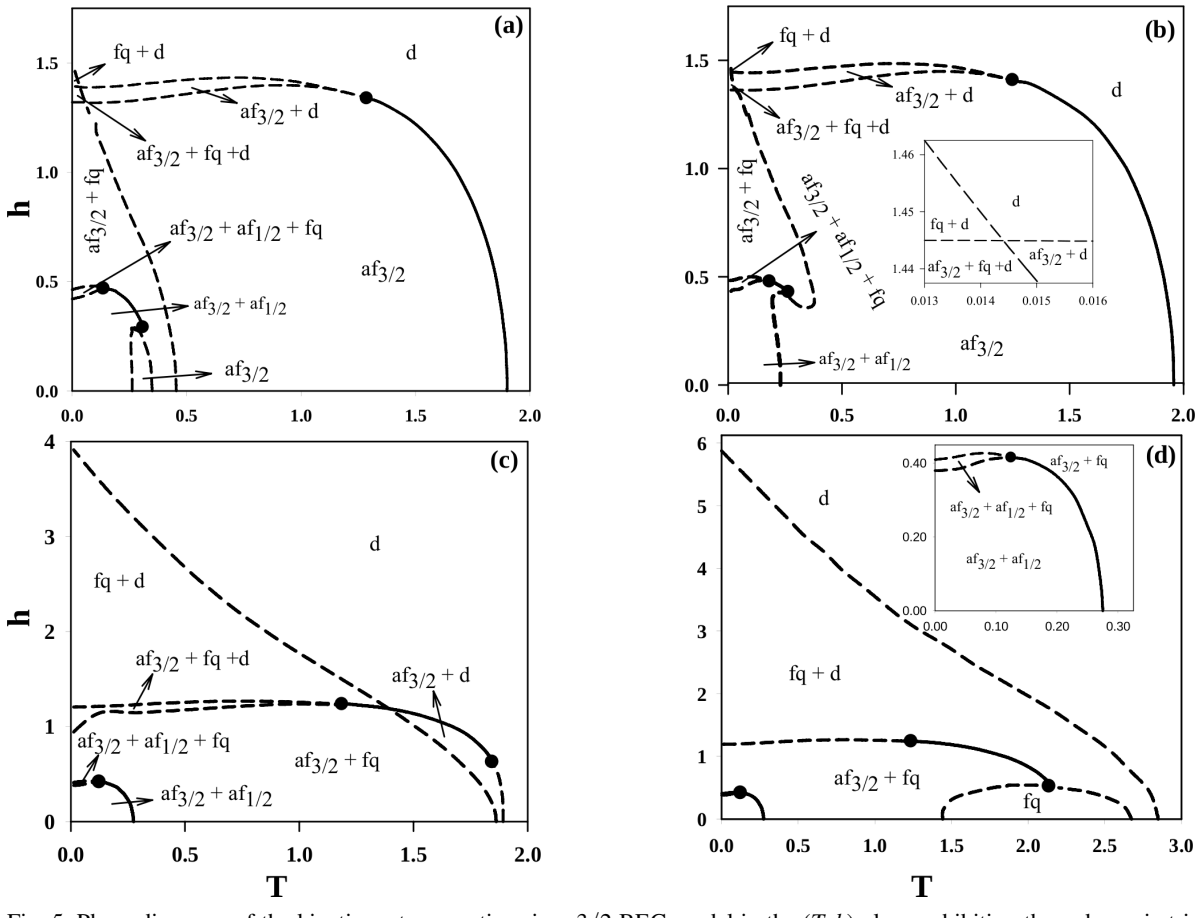

Fig. 5. Phase diagrams of the kinetic metamagnetic spin $-3/2$ BEG model in the (T,h) plane exhibiting three dynamic tricritical points. The disordered (d), antiferromagnetic $-3/2$ ($af_{3/2}$), ferroquadrupolar (fq) and six different regions coexisting phases, namely, the $af_{3/2}+af_{1/2}$, $af_{3/2}+af_{1/2}+fq$, $af_{3/2}+fq$, $af_{3/2}+d$, $af_{3/2}+fq+d$ and $fq+d$ regions, are found. Dashed and solid lines represent the first- and second-order phase transitions, respectively; the dynamic tricritical points are indicated with filled circles. (a) $k=k'=0.50$, $d=0.25$, $\alpha=-0.25$; (b) $k=k'=0.50$, $d=-0.25$, $\alpha=-0.30$; (c) $k=k'=1.00$, $d=0.025$, $\alpha=-0.10$; (d) $k=k'=1.50$, $d=0.025$, $\alpha=-0.10$.

($T_t=1.89$). In Fig. 2d, the system undergoes two successive phase transitions: the first one is a second-order phase transition from the $af_{1/2}$ phase to the fq phase ($T_{C'}=0.27$), and the second one is a first-order phase transition from the fq phase to d phase ($T_{tQ}=1.85$) for only Q_A and Q_B. Figures 2c and d imply that the system exhibits the $af_{3/2}+af_{1/2}$ region of coexisting phases for very low values of the temperature, then the $af_{3/2}+fq$ phase, then the $af_{3/2}+d$ phase and finally the d phase for very high values of the temperature (compare Figs. 2c and d, with Fig. 5c for $h=0.125$). Figures 2e–g show the behaviour of M_A, M_B, Q_A and Q_B as functions of the reduced temperature for $k=k'=0.50$, $d=-0.25$, $\alpha=-1.20$, and $h=0.75$ for three different initial values, i. e., the initial values $M_A=1.5$, $M_B=0.0$, $Q_A=1.0$, and $Q_B=-1.25$ for Fig. 2e, and $M_A=0.5$, $M_B=0.0$, $Q_A=-1.0$, and $Q_B=-1.25$ for Fig. 2f, and $M_A=0.0$, $M_B=0.0$, $Q_A=-1.25$, and $Q_B=-1.25$ for Figure 2g. The behaviour in Fig. 2e is similar to that in Fig. 2c, hence, the system undergoes the first-order phase transition from the $af_{3/2}$ phase to the fq phase ($T_t=2.34$). In Fig. 2f, the system undergoes three successive phase transitions: The first one is a second-order phase transition from the $af_{1/2}$ phase to the fq phase ($T_{C'}=0.41$), the second one is a first-order phase transition from the fq phase to the $af_{3/2}$ phase ($T_{tQ}=0.67$), and the third one is also a first-order phase transition from the

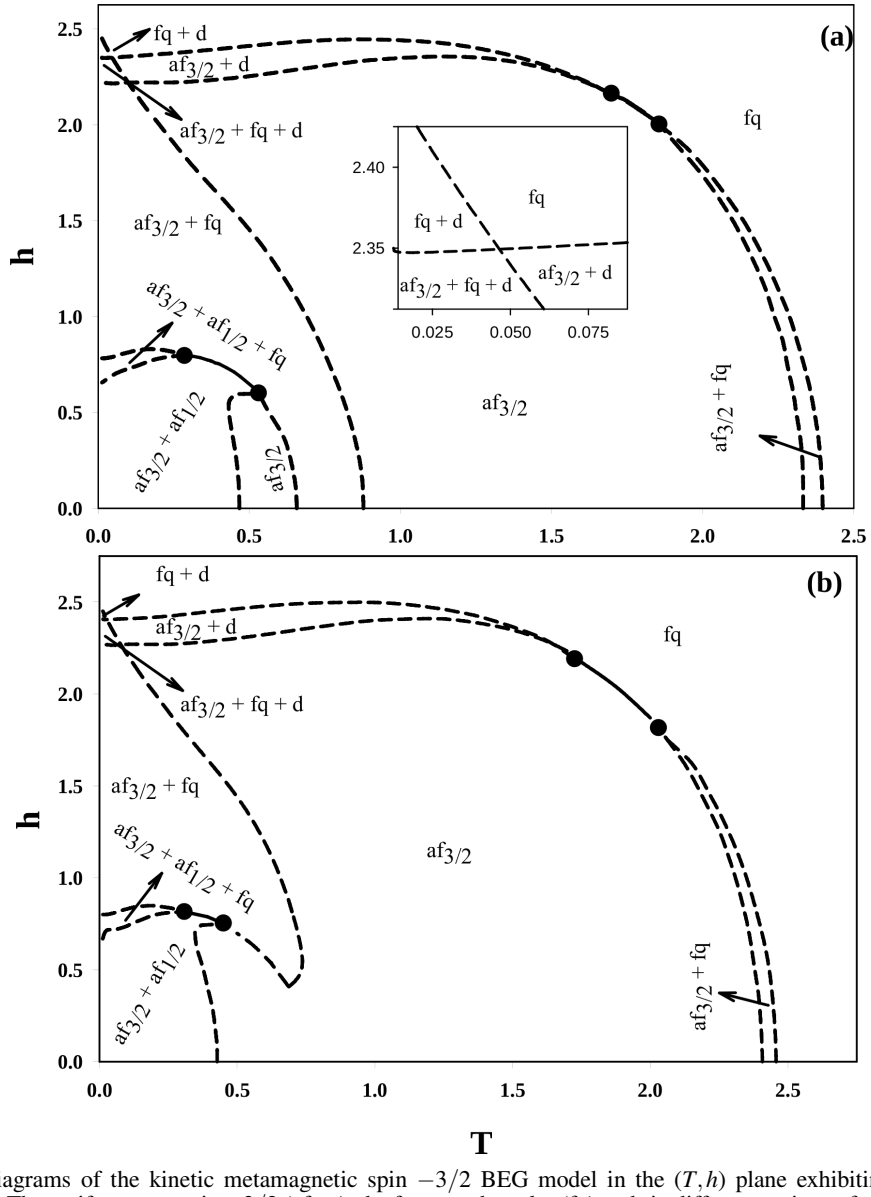

Fig. 6. Phase diagrams of the kinetic metamagnetic spin $-3/2$ BEG model in the (T,h) plane exhibiting four dynamic tricritical points. The antiferromagnetic $-3/2$ ($\mathrm{af}_{3/2}$), the ferroquadrupolar (fq) and six different regions of coexisting phases, namely, the $\mathrm{af}_{3/2}+\mathrm{af}_{1/2}$, $\mathrm{af}_{3/2}+\mathrm{af}_{1/2}+\mathrm{fq}$, $\mathrm{af}_{3/2}+\mathrm{fq}$, $\mathrm{af}_{3/2}+\mathrm{d}$, $\mathrm{af}_{3/2}+\mathrm{fq}+\mathrm{d}$ and $\mathrm{fq}+\mathrm{d}$ regions, are found. Dashed and solid lines represent the first- and second-order phase transitions, respectively; the dynamic tricritical points are indicated with filled circles. (a) $k=k'=0.50$, $d=-0.25$, $\alpha=-1.20$; (b) $k=k'=0.50$, $d=-0.25$, $\alpha=-1.25$.

$\mathrm{af}_{3/2}$ phase to the fq phase ($T_\mathrm{t}=2.31$). In Fig. 2g, the system undergoes four successive phase transitions: the first one is a first-order phase transition from the fq phase to the $\mathrm{af}_{1/2}$ phase ($T_\mathrm{t}=0.14$), the second one is a second-order phase transition from the $\mathrm{af}_{1/2}$ phase to the fq phase ($T_{C'}=0.41$), the third one is a first-order phase transition from the fq phase to the $\mathrm{af}_{3/2}$ phase ($T_{tQ}=0.67$), and the fourth one is also a first-order phase transition from the $\mathrm{af}_{3/2}$ phase to the fq phase ($T_\mathrm{t}=2.31$). These three figures imply that the system exhibits the $\mathrm{af}_{3/2}+\mathrm{af}_{1/2}+\mathrm{fq}$ coexistence region or phase for very low temperatures, then the $\mathrm{af}_{3/2}+\mathrm{af}_{1/2}$ phase, the $\mathrm{af}_{3/2}+\mathrm{fq}$ phase, the $\mathrm{af}_{3/2}$ phase, the $\mathrm{af}_{3/2}+\mathrm{fq}$ phase, and finally the fq phase for

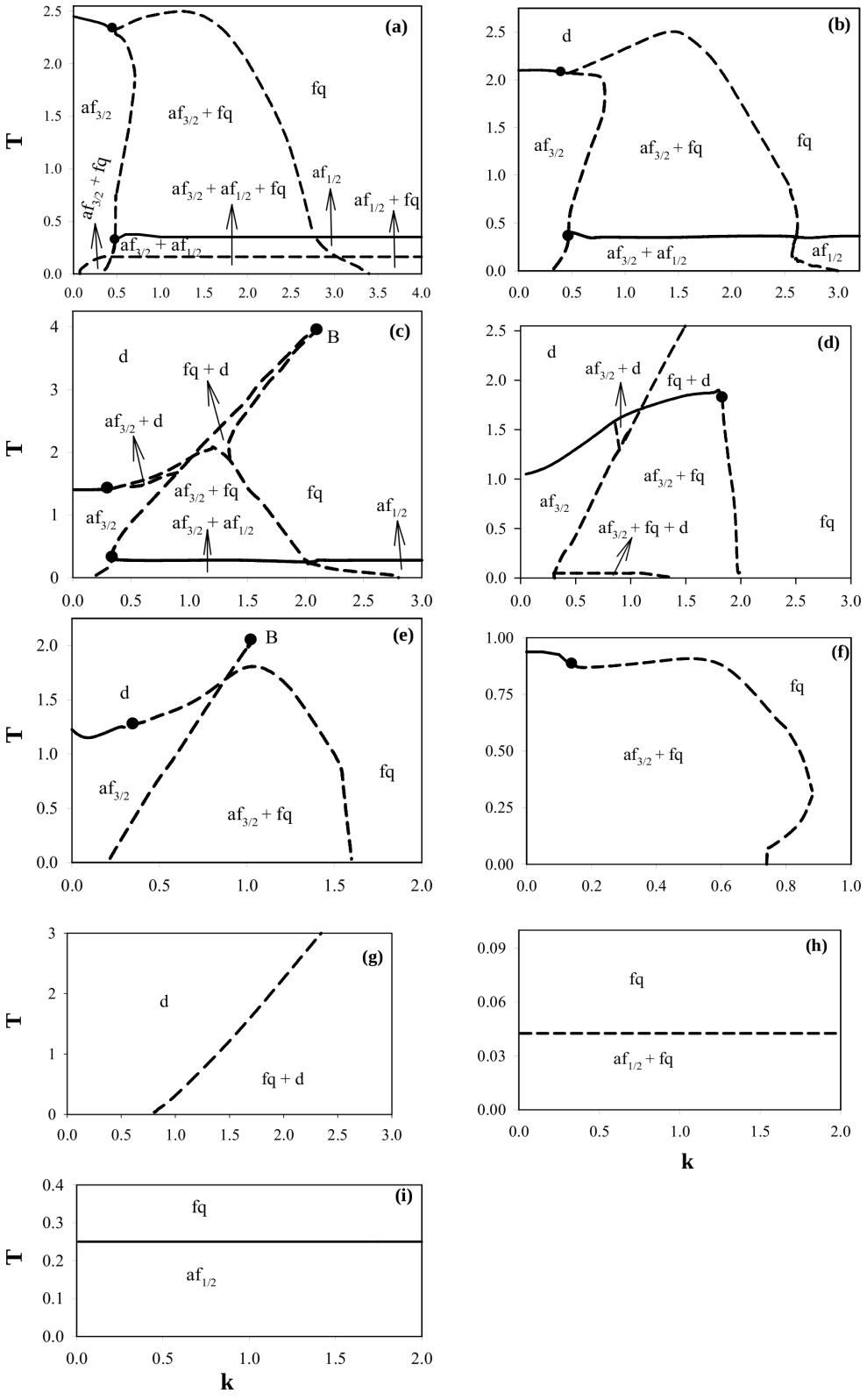
(a)
af3/2
af3/2 + fq
fq
af3/2 + af1/2 + fq
af1/2
af1/2 + fq
af3/2 + af1/2
(b)
d
af3/2
af3/2 + fq
fq
af3/2 + af1/2
af1/2
(c)
B
d
fq + d
af3/2 + d
af3/2 + fq
fq
af1/2
af3/2
af3/2 + af1/2
(d)
d
af3/2 + d
fq + d
af3/2 + fq
af3/2
af3/2 + fq + d
fq
(e)
B
d
af3/2
af3/2 + fq
fq
(f)
fq
af3/2 + fq
(g)
d
fq + d
(h)
fq
af1/2 + fq
(i)
fq
af1/2
T
k

← Fig. 7. Phase diagrams of the kinetic metamagnetic spin $-3/2$ BEG model in the (k,T) plane for several values of α, d and h. The disordered (d), antiferromagnetic $-3/2$ ($af_{3/2}$), antiferromagnetic $-1/2$ ($af_{1/2}$), ferroquadrupolar (fq) and seven different regions of coexisting phases, namely the $af_{3/2}+af_{1/2}$, $af_{1/2}+fq$, $af_{3/2}+fq$, $af_{3/2}+d$, $af_{3/2}+af_{1/2}+fq$, $fq+d$ and $af_{3/2}+fq+d$ regions, are found. Dashed and solid lines represent the first- and second-order phase transitions, respectively; the dynamic tricritical points are indicated with filled circles and the dynamic double-critical end point is represented by B. (a) $\alpha=-1.20$, $d=-0.25$, $h=0.75$; (b) $\alpha=-0.75$, $d=-0.06$, $h=0.50$; (c) $\alpha=-0.10$, $d=0.025$, $h=0.125$; (d) $\alpha=-0.10$, $d=0.025$, $h=1.00$; (e) $\alpha=-0.15$, $d=-0.06$, $h=0.75$; (f) $\alpha=-0.10$, $d=-0.25$, $h=0.75$; (g) $\alpha=-0.10$, $d=0.25$, $h=2.65$; (h) $\alpha=-0.05$, $d=-0.75$, $h=0.45$; (i) $\alpha=-0.05$, $d=-0.75$, $h=0.1875$.

very high temperatures. These facts are seen clearly in the phase diagram of Fig. 6a for $h=0.75$.

5. Phase Diagrams

Since we have obtained DPT points in Section 4, we can now present the phase diagrams of the system. The calculated phase diagrams in the (T,h) plane are presented in Figs. 3 – 6 for various values of k, k', d, and α. In these phase diagrams, the solid and dashed lines represent the second- and the first-order phase transition lines, respectively, the dynamic tricritical point is denoted by a filled circle and B represents the dynamic double-critical end point. As seen from the figures, one, two, three or four dynamic tricritical points occur depending on the interaction parameters.

Eight, two, four and two main different topological types of dynamic phase diagrams are found in Figs. 3, 4, 5 and 6, respectively. If one can investigate these phase diagrams, one can observe following interesting and main results: (1) The phase diagrams exhibit one, two, three and four dynamic tricritical points, and besides a disordered (d), three ordered phases ($af_{3/2}$, $af_{1/2}$ and fq) and seven regions of coexisting or mixed phases depending on the interaction parameters. (2) The dynamic phase boundaries are the second-order transition lines between the $af_{3/2}$ and d phases, between the $af_{3/2}+af_{1/2}$ and $af_{3/2}+fq$ phases, and between the $af_{1/2}$ and fq phases. The phase boundaries among all other phases are first-order transition lines. (3) The dynamic double-critical end point (B) separates one phase region from the other phase region, as seen Figs. 3f and h. Moreover, we observe a phase diagram in Fig. 3a, which is very similar to earlier studies of the kinetic spin $-3/2$ Ising systems [25 – 27], except that the ferromagnetic $-3/2$ ($f_{3/2}$) phase exists instead of the $af_{3/2}$ phase, also to the kinetic spin $-1/2$ Ising model [28], kinetics of a mixed spin $-1/2$ and spin -1 Ising model [29] and kinetic spin -1 Ising systems [29 – 31], but the ferromagnetic (f) phase occurs instead of the $af_{3/2}$ phase in [30 – 32]. Moreover, we also find the similar topology of phase diagram to Figs. 3b and c in [25 – 27], except that the $f_{3/2}$, $f_{3/2}+fq$, $f_{3/2}+d$ and $f_{3/2}+f_{1/2}$ phases occur instead of the $af_{3/2}$, $af_{3/2}+fq$, $af_{3/2}+d$ and $af_{3/2}+af_{1/2}$ phases, respectively. We should also mention that Figs. 3d – h and Figs. 4 – 6 are the new phase diagrams obtained by this model.

We have investigated the influence of the reduced biquadratic exchange parameter (k) and present the phase diagrams in the (k,T) plane in Figure 7. In these phase diagrams, the solid and dashed lines represent the second- and first order phase transitions, respectively. The dynamic tricritical point is indicated with a solid circle and the dynamic double-critical end point is represented by B. We obtain nine different phase diagram topologies in which six of them cannot be readily obtained from the phase diagrams in the (T,h) plane and three of them can be readily obtained from the phase diagrams in the (T,h) plane. The following main results are observed from Fig. 7:

(1) One and two dynamic tricritical points are found in Figs. 7d – f and 7a – c, respectively. Figures 7g – i do not exhibit any tricritical point. (2) Figures 7c and e contain the dynamic double critical end point. (3) The dynamic phase boundaries are the second-order transition lines between the $af_{3/2}$ and d phases, between the $af_{3/2}+af_{1/2}$ and $af_{3/2}+fq$ phases, and between the $af_{1/2}$ and fq phases. The phase boundaries among all other phases are first-order transition lines. (4) The phase boundary between the $af_{3/2}$ and d phases is a first-order line for high values of k, as seen in Figure 7e.

6. Summary and Conclusions

We have analyzed, within a mean-field approach, the stationary states of the kinetic metamagnetic spin $-3/2$ BEG model under a time-dependent oscillating external magnetic field. We used the Glauber-type stochastic dynamics to describe the time evolution of the system. We have studied the behaviour of

the time dependences of the average order parameters, namely the sublattice magnetizations or dipole moments and the sublattice quadrupole moments. We also investigated the dynamic order parameters; as a result the DPT points were calculated. We presented the phase diagrams in the (T,h) plane. We found that the behaviour of the system strongly depends on the values of k, k', d and α, and sixteen different phase diagram topologies were found. The phase diagrams exhibited besides the d, af$_{3/2}$, af$_{1/2}$, fq phases, seven coexistence regions, namely af$_{3/2}$ + af$_{1/2}$, af$_{1/2}$ + fq, af$_{3/2}$ + fq, af$_{3/2}$ + d, af$_{3/2}$ + af$_{1/2}$ + fq, fq + d and af$_{3/2}$ + fq + d, depending on the values k,k', d and α. The dynamic phase boundaries among these phases were first-order lines for most cases and second-order lines for a few cases. The system also exhibited one, two, three or four dynamic tricritical points and a dynamic double-critical end point (B) depending on k, k', d and α. We have investigated the influence of the biquadratic exchange constant and have obtained nine different phase diagram topologies in the (k,T) plane in which six of them could not be readily obtained from the phase diagrams in the (T,h) plane and three of them could be readily obtained from the phase diagrams in the (T,h) plane.

We should also mention that the existence of the dynamical tricritical point (TCP) is restricted to mean-field studies only [33 – 36]. The fluctuation destroys the existence of the dynamic TCP. For example, Acharyya [35] has done a work to establish the appearance of the dynamic TCP accompanied by stochastic resonance, but Korniss et al. [36] showed that this may be a finite size effect. Recently, Acharyya and Acharyya [37] found that the dynamic TCP may appear in mean-field studies. Hence, all these studies concluded that the dynamic TCP is observed only in mean-field studies.

It should be also mentioned that since the mean-field equations correspond to extrema in the free energy, (8) – (11) might not correspond to a global minimum of the free energy. Therefore, there is a strong possibility that at least some of the first-order transitions seen in the phase diagrams are very likely artifacts of the approximation due to its limitations, such as the correlations of spin fluctuations have not be been considered. However, this mean-field dynamic study suggests that the metamagnetic spin $-3/2$ BEG model gives more interesting dynamic phase diagrams; hence, a further with more accurate techniques such as dynamic Monte Carlo simulations or the renormalization group calculations would be worthwhile.

Finally, we should emphasize that the present study is primarily of theoretical interest. We hope that this study is able to stimulate theoretical physicists to continue to get more theoretical results about the metamagnetic systems. We also hope it may give some light for experimental works.

Acknowledgements

This work was supported by the Scientific and Technological Research Council of Turkey (TÜBİTAK), Grant No. 105T114, and by Erciyes University Research Funds, Grant No. FBA-06-01.

[1] M. Keskin, O. Canko, and M. Kırak, Phys. Status Solidi (b) **244**, 3775 (2008).
[2] R. J. Glauber, J. Math. Phys. **4**, 294 (1963).
[3] P. M. Levy, P. Morin, and D. Schmitt, Phys. Rev. Lett. **42**, 1417 (1979); J. Kötzler and G. Raffius, Z. Phys. B **38**, 139 (1980).
[4] R. Aléonard and P. Morin, Phys. Rev. B **19**, 3868 (1979).
[5] P. Morin, J. Rouchy, and D. Schmitt, Phys. Rev. B **17**, 3684 (1978).
[6] P. M. Levy, J. Phys. C **6**, 3545 (1973).
[7] J. Kötzler, G. Raffius, A. Loidl, and C. M. E. Zeyen, Z. Phys. B **35**, 125 (1979).
[8] C. Jaussaud, P. Morin, and D. Schmitt, J. Magn. Magn. Mater. **22**, 98 (1980).
[9] A. Loidl, K. Knorr, M. Müllner, and K. H. J. Buschow, J. Appl. Phys. **52**, 1433 (1981).
[10] H. H. Chen and P. M. Levy, Phys. Rev. B **7**, 4267 (1973); M. Tanaka and I. Mannari, J. Phys. Soc. Jpn. **41**, 3 (1976).
[11] K. G. Chakraborty, Phys. Rev. B **29**, 1454 (1984); J. W. Tucker, J. Phys. C **21**, 6215 (1988); K. G. Chakraborty, J. Phys. C **21**, 2911 (1988); A. F. Siqueira and I. P. Fittipaldi, Phys. Rev. B **31**, 6092 (1985); K. G. T. Chakraborty and T. Morita, Physica A **129**, 415 (1985).
[12] M. Keskin, M. Arı, and P. H. E. Meijer, Physica A **157**, 1000 (1989); M. Keskin and P. H. E. Meijer, J. Chem. Phys. **85**, 7324 (1986).
[13] J. Sivardiére and M. Blume, Phys. Rev. B **5**, 1126 (1972).
[14] O. Özsoy and M. Keskin, Physica A **319**, 404 (2003); O. Canko and M. Keskin, Int. J. Mod. Phys. B **20**, 455 (2006).
[15] D. K. Ray and Sivardiére, J. Phys. Rev. B **18**, 1401

(1978); W. Phystasz, Phys. Rev. B **37**, 9813 (1988); M. Dudzinski, G. Fath, and J. Sznajd, Phys. Rev. B **59**, 13764 (1999).
[16] P. Morin and D. Schmitt, Phys. Rev. B **27**, 4412 (1983).
[17] K. Harada and N. Kawashima, Phys. Rev. B **65**, 052403 (2002).
[18] M. M. P. de Azevedo, C. Binek, J. Kushauer, W. Kleemann, and D. Bertrand, J. Magn. Magn. Mater. **140**, 1557 (1995); W. Selke and S. Dasgupta, J. Magn. Magn. Mater. **147**, L245 (1995); W. Selke, Z. Phys. B **145**, 150 (1996); M. Zukovic, A. Bobak, and T. Idogaki, J. Magn. Magn. Mater. **188**, 52 (1998); **192**, 363 (1999); H. A. Katoria, K. Katsumata, and M. Katoria, Phys. Rev. B **54**, R9620 (1996); E. B. Filho and J. de Sousa, Phys. Lett. A **323**, 9 (2004); D. C. de Oliveira, A. A. P. da Silva, D. F. de Albuquerque, and A. S. de Arruda, Physica A **386**, 205 (2007); H. Miao, G. Wei, J. Liu, and J. Geng, J. Magn. Magn. Mater. **320**, 2172 (2008) and references therein.
[19] B. K. Chakrabarti and M. Acharyya, Rev. Mod. Phys. **71**, 847 (1999); T. Yasui, H. Tutu, M. Yamamoto, and H. Fujisaka, Phys. Rev. E **66**, 036123 (2002); A. Chatterjee and B. K. Chakrabarti, Phase Trans. **77**, 581 (2004); M. Acharyya, Phys. Rev. E **69**, 027105 (2004); M. Acharyya, Int. J. Mod. Phys. C **16**, 1631 (2005); E. Machado, G. M. Buendía, P. A. Rikvold, and R. M. Ziff, Phys. Rev. E **71**, 016120 (2005); T. Vojta and M. Y. Lee, Phys. Rev. Lett. **96**, 035701 (2006); V. Popkov and J. Krug, Phys. Rev. B **73**, 235430 (2006); M. Keskin, O. Canko, and B. Deviren, Phys. Rev. E **74**, 011110 (2006); O. Canko, B. Deviren, and M. Keskin, J. Phys.: Condens. Matter **18**, 6635 (2006); M. Keskin, O. Canko, and M. Kırak, J. Stat. Phys. **127**, 359 (2007); G. Berkolaiko and M. Grinfeld, Phys. Rev. E **76**, 061110 (2007); D. T. Robb, P. A. Rikvold, A. Berger, and M. A. Novotny, Phys. Rev. E **76**, 021124 (2007); B. Deviren, M. Keskin, and O. Canko, Comput. Phys. Commun. **178**, 420 (2008); B. V. Petukhov, Phys. Rev. E **77**, 026601 (2008); S. W. Kim and J. D. Noh, Phys. Rev. Lett. **100**, 118702 (2008) and references therein.
[20] Q. Jiang, H. N. Yang, and G. C. Wang, Phys. Rev. B **52**, 14911 (1995); W. Kleemann, T. Braun, J. Dec, and O. Petracic, Phase Trans. **78**, 811 (2005); D. T. Robb, Y. H. Xu, O. Hellwing, A. Berger, M. A. Novotny, and P. A. Rikvold, Meeting of the American Physical Society, March 13 – 17, 2006, Baltimore, MD, USA; D. T. Robb, Y. H. Xu, O. Hellwing, J. McCord, A. Berger, M. A. Novotny, and P. A. Rikvold, Phys. Rev. B **78**, 134422 (2008).
[21] Z. A. Samoilenko, V. D. Okunev, E. I. Pushenko, V. A. Isaev, P. Gierlowski, K. Kolwas, and S. J. Lewandowski, Inorg. Mater. **39**, 836 (2003).
[22] M. C. Cross and P. C. Hohenberg, Rev. Mod. Phys. **65**, 851 (1993).
[23] A. S. Mikhailov and G. Ertl, Science **272**, 1596 (1996).
[24] E. Ma, P. Bellon, M. Atzmon, and R. Trivedi (Eds.), Phase Transformations Systems Driven Far from Equilibrium, Materials Research Society Symposium Proceedings **481**, 631 (1998).
[25] T. W. B. Kibble, J. Phys. A **9**, 1387 (1976); Phys. Rep. **67**, 183 (1980).
[26] J. C. Xavier, F. C. Alcaraz, D. P. Lara, and J. A. Plascak, Phys. Rev. B **57**, 11575 (1998); A. Bakchich and M. El Bouziani, J. Phys.: Condens. Matter **13**, 91 (2001).
[27] M. Keskin, O. Canko, and B. Deviren, Phys. Rev. E **74**, 011110 (2006).
[28] O. Canko, B. Deviren, and M. Keskin, J. Phys.: Condens. Matter **18**, 6635 (2006).
[29] M. Keskin, O. Canko, and M. Kırak, J. Stat. Phys. **127**, 359 (2007).
[30] T. Tomé and M. J. Oliveira, Phys. Rev. A **41**, 4251 (1990).
[31] G. M. Buendía and E. Machado, Phys. Rev. E **58**, 1260 (1998).
[32] M. Keskin, O. Canko, and U. Temizer, Phys. Rev. E **72**, 036125 (2005).
[33] M. Keskin, O. Canko, and E. Kantar, Int. J. Mod. Phys. C **17**, 1239 (2006).
[34] M. Keskin, O. Canko, and U. Temizer, Int. J. Mod. Phys. C **17**, 1717 (2006).
[35] M. Acharyya, Phys. Rev. E **59**, 218 (1999).
[36] G. Korniss, P. A. Rikvold, and M. A. Novotny, Phys. Rev. E **66**, 056127 (2002).
[37] M. Acharyya and A. B. Acharyya, Commun. Comput. Phys. **3** 397 (2008).